Broadband emission in Er–Tm codoped Al_2O_3 films: The role of energy transfer from Er to Tm

Zhisong Xiao
Laser Processing Group, Instituto de Optica, CSIC, Serrano 121, 28006 Madrid, Spain and Department of Physics, School of Science, Beijing University of Aeronautics and Astronautics, Beijing 100083, China

R. Serna[a] and C. N. Afonso
Laser Processing Group, Instituto de Optica, CSIC, Serrano 121, 28006 Madrid, Spain

(Received 3 May 2006; accepted 29 November 2006; published online 7 February 2007)

Er–Tm codoped a-Al_2O_3 thin films prepared by alternate pulsed laser deposition show a broad photoluminescence band with two characteristic peaks at 1540 and at 1640 nm, respectively, related to Er^{3+} and Tm^{3+} emissions. Two series of films have been prepared. For the first series, the Tm concentration [Tm] has been increased while keeping constant the Er concentration [Er]. The results show that the photoluminescence intensity at 1640 nm (I_{1640}) to that at 1540 nm (I_{1540}) decreases and that at 1640 nm (I_{1640}) increases, i.e., the (I_{1640}/I_{1540}) ratio increases as [Tm] is increased. For [Tm]/[Er]=3, a fairly flat emission spectrum ($I_{1640}/I_{1540}\sim 1$) with a full width at half maximum of 230 nm is achieved. For the second series both [Tm] and [Er] are increased while keeping the [Tm]/[Er] ratio constant. The I_{1640}/I_{1540} ratio tends to be constant with a full width at half maximum of 150 nm. The lifetime values decrease in all cases as [Tm] increases. The evolution of the I_{1640}/I_{1540} and lifetimes as a function of [Tm] as well as the analysis of the latter considering Er as a donor and Tm as an acceptor evidence that there is an efficient energy transfer from Er^{3+} to Tm^{3+}. These results suggest that enhanced performance with a flat broadband emission useful for planar integrated devices is achievable by further dopant engineering in the nanoscale. © *2007 American Institute of Physics*. [DOI: 10.1063/1.2433748]

I. INTRODUCTION

Integrated optoelectronic circuits require the development of light sources and optical amplifiers in planar waveguides. Rare earth (RE) doping of dielectrics allows suitable materials for these applications.[1,2] Moreover, there is a great effort to develop planar devices for wavelength division multiplexing (WDM) in access and local networks, that require the design and implementation of broadband optical amplifiers covering the range from 1.4 to 1.6 μm, in addition to the present silica based erbium (Er) doped amplifiers (1530–1630 nm).[3,4] In principle, it is possible to use a configuration of independent amplifiers in order to cover different wavelength ranges. However, this configuration will lead to an increased complexity in the network as well as to a gain spectrum that is not likely to be continuous. The use of more than one kind of a RE ion in a single integrated device is an interesting alternative approach to develop broadband integrated optical amplifiers. The emission of thulium ions (Tm^{3+}) offers a promising complement to that of Er^{3+} due to their emission bands around 1.47 and 1.6–2.1 μm.[5,6] Therefore Tm doping and Er–Tm codoping have intensively been studied for materials suitable for fiber amplifiers[5–8] and to a much less extent in thin films for planar devices.[9,10]

When doping with Tm^{3+} the choice of a suitable host material is essential. Due to its electronic structure, silica and most silica based glasses are not as suitable for Tm^{3+} as they are for Er^{3+} due to their relative high maximum phonon energy ($\sim$1100 cm^{-1}) that inhibits the emission at 1.47 μm. As a consequence significant effort has been directed to the research of Tm-doped fluorides due to their low phonon energies ($\sim$580 cm^{-1}) compared to silica based glasses.[5,11] However, considering the rather poor chemical durability of most fluoride glasses the development of more robust glasses such as oxides with sufficiently low maximum phonon energy is necessary. For this reason tellurite[7] and aluminate glasses[12] have recently been explored as potential materials for future near infrared light sources and amplifiers. An attractive alternative material host for integrated optical circuits based on the silica-on-silicon approach is the amorphous aluminum oxide (a-Al_2O_3), that shows a moderate maximum phonon energy ($\sim$870 cm^{-1}) (Ref. 13) as well as a high refractive index compared to SiO_2, thus making possible small device structures.[14]

In previous works we have shown that alternate pulsed laser deposition (PLD) of the host (a-Al_2O_3) and the RE dopant (Er and Yb) can be used to obtain artificial structures in which the RE concentration and the ion-ion separation are controlled in the nanometer scale.[15,16] This approach has recently been applied to Er and Tm codoping and a broad emission band in the 1.4 to 1.7 μm has been achieved for a specific configuration.[17] The aim of this work is to determine the dependence of the emission band in terms of its intensity, width, and lifetime on the Tm and Er concentration and dis-

[a]Electronic mail: rserna@io.cfmac.csic.es

TABLE I. Summary of the production parameters and the RE concentration of the films studied in this work.

Sample	Number of Tm layers/cycle	Er–Er layer separation (nm)	Number of cycles	Total [Tm] (10^{20} cm^{-3})	Total [Er] (10^{20} cm^{-3})	[Tm]/[Er]
Er only	0	6	50	⋯	0.72	⋯
Tm only	1	⋯	200	2.84	⋯	⋯
f(Tm)-1[a]	1	6	50	0.72	0.72	1
f(Tm)-2	2	6	50	1.43	0.72	2
f(Tm)-3	3	6	50	2.15	0.72	3
f(Tm)-5	5	6	50	3.57	0.72	5
f(RE)-50[a]	1	6	50	0.72	0.72	1
f(RE)-75	1	4	75	1.12	1.12	1
f(RE)-150	1	2	150	2.19	2.19	1
f(RE)-200	1	1.5	200	2.82	2.82	1
f(RE)-300	1	1	300	4.33	4.33	1

[a]*f*(Tm)-1 and *f*(RE)-50 are the same sample, that forms part of both series. The data are repeated in order to facilitate comparison within each series.

tribution, in order to both optimize the emission efficiency and to understand the energy transfer mechanisms between Tm^{3+} and Er^{3+}.

II. EXPERIMENT

An ArF excimer laser ($\lambda = 193$ nm and $\tau = 520$ ns full width at half maximum) was used to alternately ablate Al_2O_3 and RE (Er and Tm) targets. The laser was focused at the targets in order to achieve an average laser energy density of 2 mJ cm^{-2}. All the films have been designed to have a total thickness of ~300 nm.

Two series with different RE distributions and concentrations have been prepared. In the *f*(Tm) series the Er concentration is constant and the Tm concentration ([Tm]) is varied by increasing the number of Tm layers inserted among two consecutive Er layers, and thus the Tm to Er concentration ratio ([Tm]/[Er]) is increased. The Er–Er in-depth separation is kept constant and equal to 6 nm. The number (n_T) of Tm layers between two consecutive Er layers has been designed to be 1, 2, 3, and 5 and, in each case, they are evenly distributed in depth. The resulting films thus have a multilayerlike structure that can schematically be described from bottom to top as $[(Al_2O_3/Tm)n_T/Al_2O_3/Er]\times 50$, 50 being the number of cycles. Further details on the *f*(Tm) series growth can be found in Ref. 17. In the *f*(RE) series, the Tm to Er concentration ratio ([Tm]/[Er]) was kept constant by depositing one Tm layer per Er layer ($n_T = 1$) and varying the number of cycles. The complete deposition sequence involves in this case an *a*-Al_2O_3 layer followed by a number n_{RE} of pairs of Er–Tm layers (cycles). The structure of these films can thus be described from bottom to top as $[Er/Al_2O_3/Tm/Al_2O_3]\times n_{RE}$ where n_{RE} has been varied from 50 to 300, and the layers have been evenly distributed throughout the film depth. Two reference films only doped with Er or Tm have also been prepared. They have an Er–Er layer separation of 6 nm [similarly to this separation in series *f*(Tm)] and a Tm–Tm layer separation of 1.5 nm. Table I summarizes the main deposition parameters for each series.

The Er and Tm concentrations were measured by Rutherford backscattering spectrometry (RBS) using a 2.0 MeV He^+ beam and a scattering angle of 165°. From the RBS analysis it is seen that the average areal density of *a*-Al_2O_3 is $\sim 2.7\times 10^{18}$ cm^{-2}, observed variations being within 10%. This corresponds to a film thickness of 310 nm assuming a density for *a*-Al_2O_3 of 8.7×10^{22} cm^{-3},[18] that is in excellent agreement with the designed thickness. The total Er areal density in the Er-only doped film is $\sim 2.2\times 10^{15}$ cm^{-2} that can be assumed to be also the Er areal density in all films in the *f*(Tm) series. The areal density of Tm in the film only doped with Tm is also 2.2×10^{15} that leads to a Tm areal density per cycle in the *f*(Tm) series ranging from this value up to 1.1×10^{16} cm^{-2}. The average Er and Tm concentrations in codoped films of the series *f*(Tm) is 7.2×10^{19} cm^{-3} for Er and between 7.9×10^{19} and 3.6×10^{20} cm^{-3} for Tm, as has been discussed in Ref. 17. For the *f*(RE) series, the average Er and Tm concentrations are almost in the same range 7.2×10^{19} to 4.3×10^{20} cm^{-3}. The specific value in each film has been included in Table I.

Photoluminescence (PL) measurements were performed at room temperature using the experimental setup described in earlier work. Pumping was performed using a Ti:sapphire laser beam at 794 nm. This wavelength corresponds to the absorption band of the $^3H_6-{}^3H_4$ transition for the Tm^{3+} ions and to the $^4I_{15/2}-{}^4I_{9/2}$ transition for the Er^{3+} ions. Both ions can thus be excited by direct absorption at this wavelength, enabling a direct comparison of results obtained in codoped films to those obtained for Er-only and Tm-only doped films. Finally, the luminescence decay curves at the peaks of the emission spectra were averaged and recorded with a digital oscilloscope to determine the lifetimes.

In a previous work,[19] the PL emission for a Er–Tm codoped film [*f*(Tm)−1 or *f*(RE)−50] has been reported to be optimum after step annealing for 1 h at 600 °C, followed by annealing during an hour at 650 °C in air. The study of the PL response as a function of the annealing temperature has yielded the same conclusion for all codoped films described in Table I, and thus results will only be presented for films after this annealing procedure.

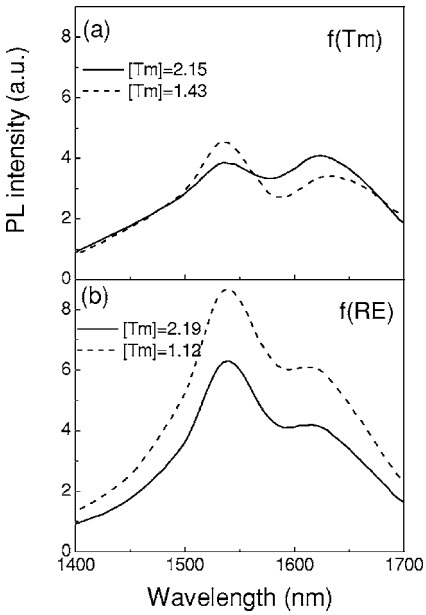

FIG. 1. PL spectra of Er–Tm codoped films: (a) (…)f(Tm)-2 and (—)f(Tm)-3 and (b) (…)f(RE)-75 and (—)f(RE)-150.

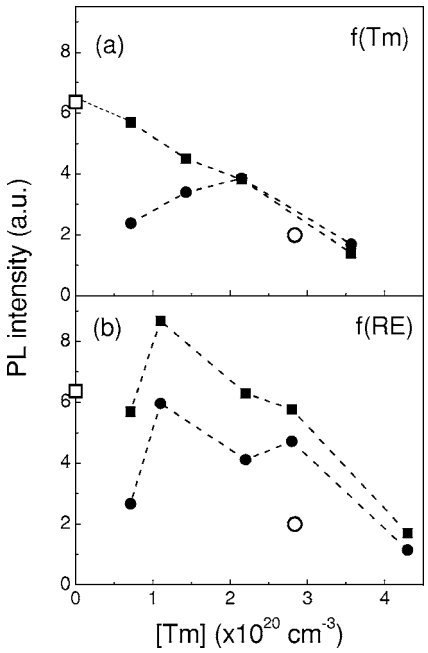

FIG. 2. PL intensity at 1540 nm (■) and 1640 nm (●) of Er–Tm codoped films as a function of the Tm concentration for (a) f(Tm) and (b) f(RE) series. The PL intensities at 1540 nm (□) for the Er-only doped film and 1640 nm (○) for the Tm-only doped film are included for comparison.

III. RESULTS

Figure 1 shows representative PL spectra for the Er–Tm codoped films of both f(Tm) and f(RE) series. The spectra corresponding to the Er-only and Tm-only reference films can be found in Ref. 17. All spectra of Er–Tm codoped films show the characteristic emission peak at 1540 nm related to the transition from the first excited state to the ground state of Er^{3+}: ${}^4I_{13/2}-{}^4I_{15/2}$. In addition a second emission peak in the range of 1620–1640 nm is always observed. This peak is most likely originated from the short wavelength band edge emission of Tm^{3+}: ${}^3F_4-{}^3H_6$. This transition is known to lead to a broad emission band that usually peaks around 1800 nm, the specific value depending on the host material. The observation of the emission at relatively short wavelengths ($\leqslant$1640 nm) is consistent with the fact that Tm^{3+} has a strong coupling to its surrounding and, thus, the transition is inhomogeneously broadened. This interpretation is supported by the reports on the especially large energy spread of the individual stark components of the ${}^3H_6$ levels for germano- and alumino-silicate glasses[20] and emission at 1630 nm for a fluorine Tm-doped crystal.[21]

The broad emission bands observed in Fig. 1 are thus the result of simultaneous emission of Er^{3+} and Tm^{3+}. The PL spectra for the f(Tm) series [Fig. 1(a)] shows that the intensity balance of the two peaks depends on the Tm concentration, leading to a fairly flat emission profile over a wide spectral range for the film having [Tm]=2.15 $\times 10^{20}$ at. cm^{-3}. The PL spectra of films in the f(RE) series [Fig. 1(b)] show a broad band with two peaks similar to the spectra from the f(Tm) series. However, the shape does not depend on the RE (Er and Tm) concentration in this case.

Figure 2 shows the evolution of the PL intensity peaks at 1540 and 1640 nm for both series of codoped films as a function of the Tm concentration. Data obtained in the Er-only and Tm-only doped films are included for comparison. For the f(Tm) series, the intensity of the emission at 1540 nm decreases following a linear trend [Fig. 2(a)] as the Tm concentration increases whereas that at 1640 nm it first increases when the Tm concentration increases up to 2.2 $\times 10^{20}$ cm^{-3} and then decreases.[17] For the f(RE) series [Fig. 2(b)], both PL peaks follow the same trend: The intensity first increases for a concentration up to 1.1×10^{20} cm^{-3} and then decreases as the Tm concentration increases further. Note that the PL intensity at 1540 nm for the f(Tm) series is always lower than that of the Er-only doped film, whereas for the f(RE) series it is always comparable to that of the Er-only doped film and only becomes significantly lower for the film with the highest Tm (or Er) concentration (4.3 $\times 10^{20}$ cm^{-3}).

The PL intensity emission at 1640 to 1540 nm ratio and the full width at half maximum (FWHM) of the spectra have been plotted in Fig. 3 as a function of the Tm concentration. It is shown that for the f(Tm) series [Fig. 3(a)], the PL intensity ratio increases nearly linearly as the Tm concentration increases, this ratio becoming equal to unity for a Tm concentration of 2.2×10^{20} cm^{-3} [the spectrum is plotted in Fig. 1(a)]. Instead, Fig. 3(b) shows that the PL intensity ratio first increases for a Tm concentration of 1.1×10^{20} cm^{-3} and then remains constant at ~0.7 for the f(RE) series. Both series of codoped films show a broad emission band in the range of 1.4–1.7 μm with a FWHM always larger than 100 nm and thus with values that are comparable or higher than those reported for Er–Tm codoped silicate and tellurite fibers.[7,8] The FWHM increases from 125 up to 230 nm for the highest Tm concentration in the f(Tm) series. Instead, it increases from 125 to a constant value around ~150 nm for Tm (or Er) concentrations higher than 1×10^{20} cm^{-3} in the f(RE) series.

Figure 4 shows the lifetimes measured in the codoped

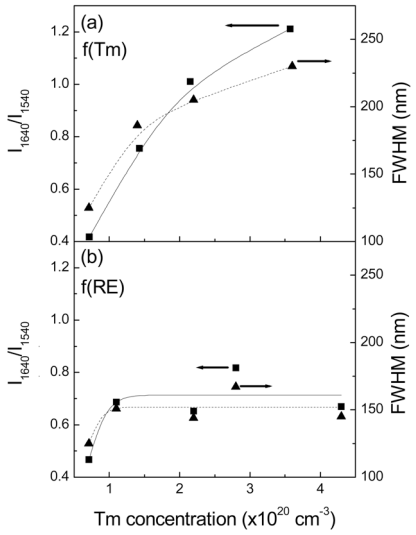

FIG. 3. (■) PL intensity at 1640 nm to 1540 nm ratio and (▲) the FWHM of the band emission as a function of the Tm concentration for (a) f(Tm) and (b) f(RE) series.

films. For comparison, results obtained in the Er-only and Tm-only doped films are also included. The results are very similar for the two studied series of films showing that the lifetime at both spectral peaks (1540 and 1640 nm) decrease as both the Tm concentration and the total RE concentration increase. The maximum value of the lifetime at 1540 nm (3.42 ms) in both series corresponds to the lifetime of the Er-only doped film. Instead, the minimum value of the lifetime at 1640 nm (0.29 ms) is close to that of the Tm-only doped film. The results thus show that the lifetime can be significantly increased (a factor of 6) by decreasing the Tm concentration.

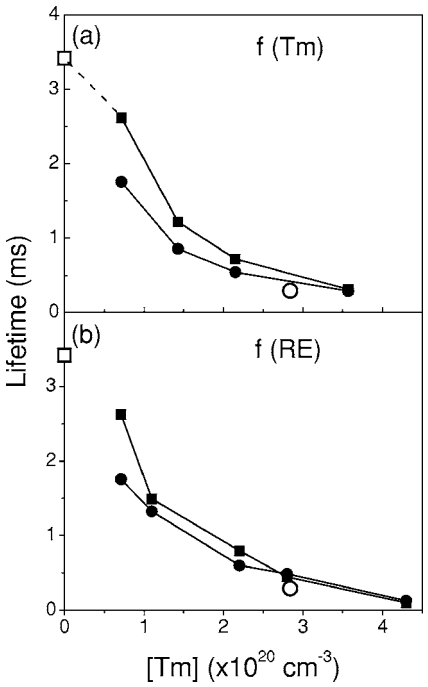

FIG. 4. PL lifetime (■) at 1540 nm and (●) at 1640 nm of the emission of Er–Tm codoped films as a function of the Tm concentration for (a) f(Tm) and (b) f(RE) series. The PL lifetimes at 1540 nm (□) for the Er-only doped film and at 1640 nm (○) for the Tm-only doped film are included for comparison.

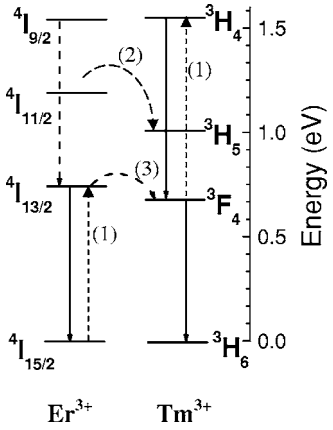

FIG. 5. Energy-level diagram of Er^{3+} and Tm^{3+} ions.

IV. DISCUSSION

The results clearly show that Er–Tm codoped a-Al_2O_3 films provide a broad emission band from 1450 to 1650 nm when using a single source of excitation at 794 nm. The specific spectral response depends on both the [Tm]/[Er] concentration ratio [series f(Tm)] and the total rare earth ion concentration [series f(RE)]. For the discussion we will follow the energy level diagram of Er^{3+} and Tm^{3+} ions schematically shown in Fig. 5.

The analysis of the results for the first series f(Tm) shows that when the Tm concentration is increased while keeping the Er concentration constant the Er^{3+} related emission intensity at 1540 nm due to the $^4I_{13/2} \rightarrow {}^4I_{15/2}$ transition always decreases as the Tm concentration increases. Furthermore, the lifetime of the 1540 nm emission decreases as the Tm concentration increases (Fig. 4). The fact that Tm codoping reduces the Er^{3+} related luminescence intensity and lifetime indicates that Tm^{3+} introduces nonradiative decay routes for excited Er^{3+} ions that can be related to energy transfer processes from Er^{3+} to Tm^{3+} ions. This is an important observation since it points out that the performance of a codoped system is substantially different than that of cascaded Er and Tm devices.

The PL intensity of the emission at 1640 nm due to the Tm^{3+} related $^3F_4 \rightarrow {}^3H_6$ transition increases as the Tm concentration is increased up to 2.15×10^{20} cm^{-3}. Moreover the lifetime of the 1640 nm emission for Tm concentrations lower than 2.15×10^{20} cm^{-3} can be higher than the value reported for this transition in silica based materials which is of the order of 400 μs.[9,22] The increase of the 1640 nm emission intensity as the Tm concentration increases has also been reported for Er–Tm codoped tellurite glasses, however, the real variation of the Er related emission intensity is not evident since all shown emission spectra were normalized to that at the Er emission peak wavelength. For the case of the Er–Tm codoped silicon-rich silicon oxide a similar decrease of the Er^{3+} related emission at 1540 nm by the presence of Tm^{3+} has been reported. However, in that case it was observed that the Tm^{3+} related PL intensity due to the $^3F_4 \rightarrow {}^3H_6$ Tm^{3+} transition was not affected by the presence of Er^{3+}.[9,22] This is not the case for the Er–Tm codoped a-Al_2O_3 since the PL intensity of codoped films at 1640 nm is higher

than that of the Tm-only doped film with the same concentration (Fig. 2). Therefore for Tm concentrations up to 2.15×10^{20} cm^{-3} it seems that the Er^{3+} to Tm^{3+} energy transfer is the dominant process in a-Al_2O_3 codoped films, that results in a decrease of the 1540 nm emission and in a relative enhancement of the 1640 nm emission. For Tm concentrations higher than 2.15×10^{20} cm^{-3} the photoluminescence intensity decreases with the increase of the Tm content for both series and the lifetimes decrease significantly. At this high RE concentration, quenching mechanisms start playing a role.[23]

The processes that have previously been reported to explain Er to Tm energy transfers in other materials are the following and are schematically shown in Fig. 5:[9,7,24]

(*1*) *Cooperative upconversion process in which an excited* Er^{3+} *ion decays nonradiatively by exciting an excited* Tm^{3+} *ion from the* $^3F_4$ *to the* $^3H_4$ *state*. This mechanism is likely since the Er^{3+}:$^4I_{13/2} \rightarrow {}^4I_{15/2}$ transition is nearly resonant with the Tm^{3+}:$^3H_4 \rightarrow {}^3F_4$ transition with an energy mismatch of ~ 0.05 eV $\equiv 403$ cm^{-1}. The excited Tm^{3+} ion can then decay via the $^3H_4 \rightarrow {}^3F_4$ and $^3F_4 \rightarrow {}^3H_6$ transitions.

(*2*) *Energy transfer from the* Er^{3+}:$^4I_{11/2}$ *state to the* Tm^{3+}:$^3H_5$ *state*. This is a nonresonant process originated from deexcitation of an Er^{3+} ion that leads to the excitation of a Tm^{3+} ion that is deexcited nonradiatively from $^3H_5$ to $^3F_4$, and then relax to the ground state generating the 1640 nm emission.

(*3*) *Energy transfer from the* Er^{3+}:$^4I_{13/2}$ *state to the* Tm^{3+}:$^3F_4$ *state*. This is a quasiresonant process with an energy mismatch of ~ 0.1 eV $\equiv 806$ cm^{-1}.

In the case of the cooperative upconversion process (1), an enhancement of the emission tail at 1480 nm upon subsequent deexcitation of the Tm^{3+}, together with the enhancement of the emission at 1640 nm, should be expected. With the increase of the Tm concentration [see Fig. 1(a)] there is a clear increase of the 1640 nm emission, but comparatively there is no evidence for the enhancement of the emission at 1480 nm. Therefore for the Er–Tm a-Al_2O_3 codoped films it is unlikely that this upconversion process is taking place. Note that the situation in our a-Al_2O_3 host is quite different than in the case of the silicon-rich-oxide films, where there is no radiative emission at 1480 nm due to strong multiphonon effects in silica that results in a nonradiative transition from $^3H_4$ to $^3F_4$. This is not the case for a-Al_2O_3 where the relatively low maximum phonon energy (870 cm^{-1}) allows the observation of the radiative decay of this transition as it is clearly seen for the Tm-only doped film.

The processes (2) and (3) are in principle possible for the a-Al_2O_3 films since both imply an effective decrease of the population of Er^{3+} and thus are able to explain the observed linear decrease of the 1540 nm emission with the increase of the Tm concentration [Fig. 2(a)]. Due to the quasiresonant nature of process (3) it can be assumed that this is the most probable process. This conclusion is in agreement with what has been reported for fluoride glasses showing that the energy transfer between Er^{3+} and Tm^{3+} occurs primarily at the lowest excited states. Since the Er concentration is constant in the f(Tm) series it is possible to calculate the energy transfer efficiency from Er^{3+} to Tm^{3+}. Considering the Er^{3+} as a donor and the Tm^{3+} as an acceptor the energy transfer can be defined as $\eta_{ET} = 1 - (\tau_f / \tau_0)$, where τ_0 and τ_f are, respectively, the lifetimes in the absence and in the presence of an acceptor.[7] Taking into account the lifetimes in Fig. 4(a) the transfer efficiency increases from 23% up to 90% as the Tm concentration increases. This indicates that for the highest Tm concentration most of the Er^{3+} excitation is transferred to Tm^{3+}. This result is in agreement with Fig. 3(a) where it is seen that the 1640 nm to the 1540 nm intensity ratio increases as the Tm concentration increases.

In the f(RE) series the situation is somehow different since the Er concentration increases at the same time as the Tm concentration increases in order to keep the [Tm]/[Er] ratio constant. Therefore, as the Tm concentration increases there are more Er^{3+} ions available for both the radiative emission and the energy transfer to Tm^{3+}. The transfer efficiency in this case should be constant since the [Tm]/[Er] ratio is constant, and this is experimentally evidenced in Fig. 3(b) where it is seen that the 1640 nm to the 1540 nm intensity ratio is almost constant at ~ 0.7. This result is also consistent with the fact that the shape of the spectrum undergoes no significant changes as the total RE ion concentration is increased [see Fig. 1(b)]. Finally, the lifetime decrease of Er^{3+} ions observed for the f(RE) series is most probably due to concentration quenching processes associated to the high concentration of Er^{3+} ions. Note that for concentrations higher than 2×10^{20} cm^{-3} in a-Al_2O_3 similar lifetime values have earlier been reported for Er-only doped films.[16]

The results obtained on Er–Tm codoped a-Al_2O_3 films show that a broad emission band with a fairly flat profile over the 1450–1650 nm wavelength range and with lifetimes in the order of milliseconds can be obtained for Tm and Er concentrations around 1×10^{20} cm^{-3} and with a [Tm]/[Er] ratio around 2. As Er^{3+} is acting as a sensitizer for Tm^{3+} it has to be realized that for broadband amplifier applications the Er^{3+}–Tm^{3+} energy transfer that enhances the Tm^{3+}-related emission reduces the efficiency of the Er^{3+} related emission. It should be noted that the f(RE) series are designed in such a way that the Er^{3+} to Tm^{3+} energy transfer is optimized for every concentration since the Er- and Tm-doped layers are alternated. For the f(Tm) series the Tm^{3+}–Tm^{3+} energy transfer could instead be favored for higher concentrations since there are several Tm layers next to each other (up to 5, see Table I), and thus the intermediate Tm-doped layers might not receive an efficient energy transfer from the Er-doped layers. This might explain also why slightly higher PL intensities are found for the f(RE) series compared to the f(Tm) ones. This reasoning evidences that there is still room for further research in engineering the dopant concentration and distribution to optimize the response of the Er–Tm codoped films in order to build efficient broadband amplifiers with a uniform response over the considered spectral range.

V. CONCLUSIONS

Er–Tm codoped a-Al_2O_3 thin films under an excitation at 794 nm show a broad emission band extending in the wavelength range of 1400–1700 nm. The full width at half

maximum (FWHM) achieved varies from 125 to 230 nm depending on the RE content and [Tm]/[Er] concentration ratio. This FWHM value is comparable or higher than that reported recently for silica (90 nm) and tellurite (160 nm) fibers. The band is mainly formed by the 1640 nm emission from Tm^{3+} and the 1540 nm emission from Er^{3+}. The results evidence an efficient energy transfer from Er^{3+} to Tm^{3+} which leads to a decrease of the efficiency of the Er^{3+}-related 1540 nm emission (both in intensity and lifetime) with respect to the Er-only doped films. However, it is also shown that dopant engineering in the nanoscale opens possible routes to optimize this energy transfer for achieving a flat and broad emission band, with enough long lifetimes and with a control over the dual role of Er^{3+} as a donor for Tm^{3+} as well as an emitter.

ACKNOWLEDGMENTS

This work was supported by CICYT (Spain) under MAT2003-01490, MAT2005-06508-C02-01, and TEC2006-04538-MIC projects. One of the authors (Z.X.) acknowledges a fellowship from MEC (SB2002-0013, Spain). The authors are very grateful to I. Vickridge (INSP, France) and to the collaborative structure around SAFIR (CNRS and MENRT, France) for making possible the RBS measurements.

[1]H. Ennen, J. Schneider, G. Pomrenke, and A. Axmann, Appl. Phys. Lett. **43**, 943 (1983).
[2]A. Polman, J. Appl. Phys. **82**, 1 (1997).
[3]J. Kani, K. Hattori, M. Jinno, S. Aisawa, T. Sakamoto, and K. Oguchi, Electron. Lett. **35**, 321 (1999).
[4]S. Tanabe, N. Sugimoto, S. Ito, and T. Hanada, J. Lumin. **87**, 670 (2000).
[5]T. Komukai, T. Yamamoto, T. Sugawa, and Y. Miyajima, IEEE J. Quantum Electron. **31**, 1880 (1995).
[6]S. L. Oliveira, S. M. Lima, T. Catunda, L. A. Nunes, J. H. Rohling, A. C. Bento, and M. L. Baesso, Appl. Phys. Lett. **84**, 359 (2004).
[7]L. Huang, A. Jha, S. Shen, and X. Liu, Opt. Express **12**, 2429 (2004).
[8]H. Jeong, K. Oh, S. R. Han, and T. F. Morse, Chem. Phys. Lett. **367**, 507 (2003).
[9]S. Y. Seo, J. H. Shin, B. S. Bae, N. Park, J. J. Penninkhof, and A. Polman, Appl. Phys. Lett. **82**, 3445 (2003).
[10]K. Watanabe, H. Tamaoka, M. Fujii, and S. Hayashi, J. Appl. Phys. **92**, 4001 (2002).
[11]M. Naftaly, S. Shen, and A. Jha, Appl. Opt. **39**, 4979 (2000).
[12]B. G. Aitken, M. J. Dejneka, and M. L. Powley, J. Non-Cryst. Solids **349**, 115 (2004).
[13]M. B. Lee, J. H. Lee, B. G. Frederick, and N. V. Richardson, Surf. Sci. **448**, L207 (2000).
[14]G. N. van den Hoven, E. Snoeks, A. Polman, J. W. M. van Uffelen, Y. S. Oei, and M. K. Smit, Appl. Phys. Lett. **62**, 3065 (1993).
[15]A. Suarez-Garcia, R. Serna, M. J. de Castro, C. N. Afonso, and I. Vickridge, Appl. Phys. Lett. **84**, 2151 (2004).
[16]R. Serna, M. J. de Castro, J. A. Chaos, A. Suarez-Garcia, C. N. Afonso, M. Fernandez, andI. Vickridge, J. Appl. Phys. **90**, 5120 (2001).
[17]Z. Xiao, R. Serna, C. N. Afonso, and I. Vickridge, Appl. Phys. Lett. **87**, 111103 (2005).
[18]R. Serna, J. C. G. de Sande, J. M. Ballesteros, and C. N. Afonso, J. Appl. Phys. **84**, 4509 (1998).
[19]Z. Xiao, R. Serna, M. J. de Castro, C. N. Afonso, and I. Vickridge, Mater. Res. Soc. Symp. Proc. **866**, V5.6.1/FF5.6.1 (2005).
[20]J. R. Lincoln, W. S. Brocklesby, F. Cusso, J. E. Townsend, A. C. Tropper, and A. Pearson, J. Lumin. **50**, 297 (1991).
[21]G. Galzerano, F. Cornacchia, D. Parisi, A. Toncelli,M. Tonelli, and P. Laporta, Opt. Lett. **30**, 854 (2005).
[22]S. Y. Seo and J. H. Shin, Appl. Phys. Lett. **85**, 4151 (2004).
[23]J. R. Lincoln, W. S. Brocklesby, F. Cusso, J. E. Townsend, A. C. Tropper, and A. Pearson, J. Lumin. **50**, 297 (1991).
[24]D. C. Yeh, R. R. Petrin, W. A. Sibley, V. Madigou, J. L. Adam, and M. J. Suscavage, Phys. Rev. B **39**, 80 (1989).